

Chapter 2 PRACTICAL ASPECTS OF ACQUIRING NMR SPECTRA

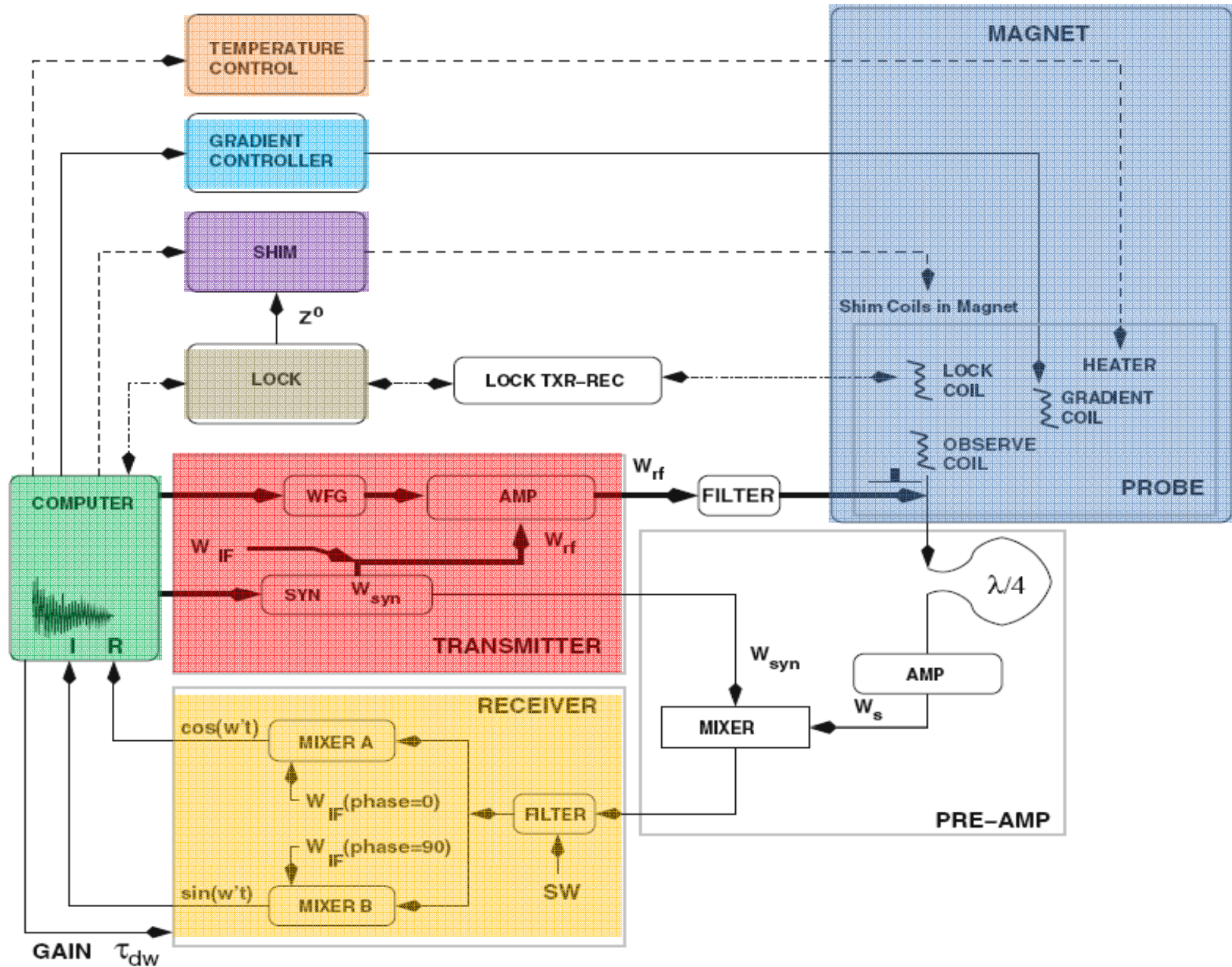


Figure 2.1. Schematic diagram of a NMR spectrometer. Circuit paths associated with the acquisition of the FID are shown in solid lines. The thicker solid lines show the path of the excitation pulse to the sample. Paths associated with control of the sample environment are shown as dotted lines. The blocks labeled 'probe' and 'pre-amp' represent discrete physical components of the spectrometer. The probe is inserted into the magnet such that the sample is placed at the center of the magnetic field (see Fig. 2.2). The pre-amp is found at the base of the magnet. The elements in the center of the diagram exist within a console adjacent to the computer. The transmitter generates the RF-pulse. W_{syn} is the frequency generated by the synthesizer. This is mixed with the intermediate frequency, W_{IF} , to produce the frequency of the B_1 field, W_{rf} , that is sent to the amplifier. The output of the amplifier can be modulated in amplitude and phase by the waveform generator (WFG). The amplified signal is subject to broadband filtering prior to entering the probe, e.g. the 1H channel would be filtered to remove frequencies that may interfere with the deuterium lock. The resonance signals from the excited spins are indicated by W_s . After amplification, this signal is reduced in frequency by W_{syn} , and signals outside of the spectral width (SW) are removed by filtering. The real (R) and imaginary (I) components are generated by mixing the signal with the intermediate frequency. The R and I components are then sampled at time points spaced by τ_{dw} , digitized, and stored separately in the computer. The gain of the receiver and the dwell time (τ_{dw}) are controlled by the computer. Magnetic field stability is controlled by the lock circuitry. The lock consists of an independent deuterium transmitter and receiver that excites and receives signals from the deuterons in the lock solvent within the sample. The current through the Z^o shim is adjusted by the lock to maintain a defined field strength.

2.1 Components of an NMR Spectrometer

2.1.1 **Magnet:** **Actively shielded** superconducting magnet.

2.1.2 **Computer:** Control, gating, pulse generation, data handling

2.1.3 **Probe:**

- Type of probe: Multinuclear (^1H , ^2D , ^{13}C , ^{15}N), broadband, triple resonance, inverse, triple resonance multiple coils etc.
- Tuning: Make sure the RLC circuitry is on resonance.
- Matching: Make sure the impedance is 50 Ohm. (The output of transmitter is usually 50 Ohm). This is reflected on the sharpness of the tuning curve on the scope.

➤ Quality factor: $Q = \nu_0 / \Delta\nu$

- For $\nu_0 = 600 \text{ MHz}$, $\Delta\nu = 1 \text{ MHz}$
then $Q = 600$.

- High Q more sensitive.

- Q is related to R , L , and C .

➤ Sensitivity: Measured with standard Compounds.

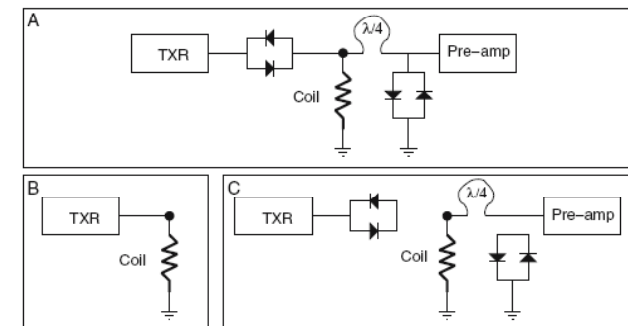
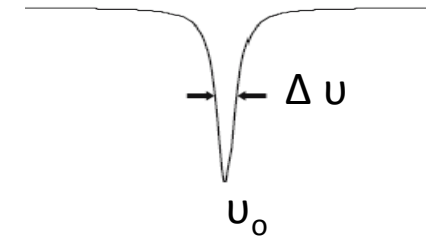
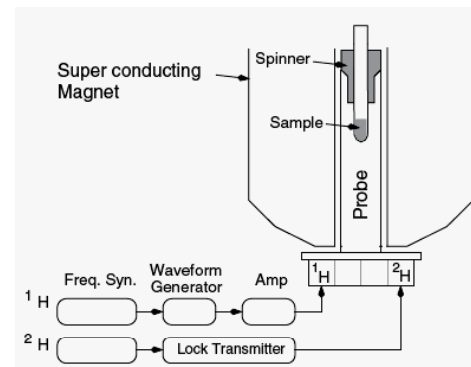
➤ Cryoprobe: With probe coil at low temperature to reduce Johnson noise (thermal noise) which increases with temperature.

2.1.4 **Pre-amplifier Module (Preamp):**

High frequency amplifier placed close to the probe to amplify microAmp signal before it decays.

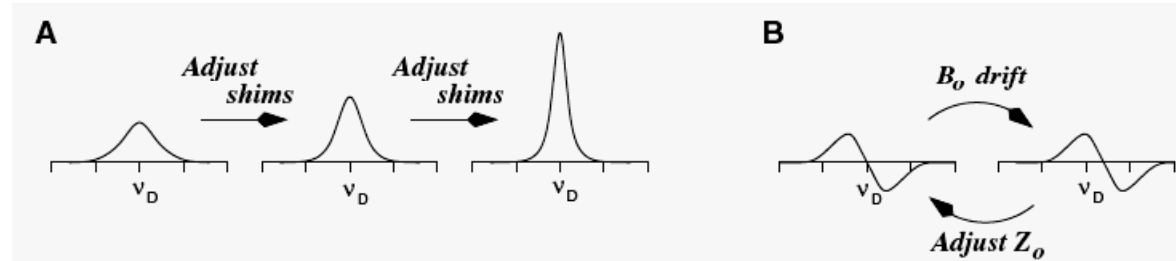
Cross diode: Conductive for high voltage (0.5V) but block low voltage RF.

$\frac{1}{4} \lambda$ cable. Cable whose length equals $\frac{1}{4}$ wavelength of RF.



2.1.5 Field frequency lock (An primitive spectrometer):

- Typical field drift: 1-10 Hz/hr. Need to be compensated by external field in Z-direction.
- This is accomplished with a field frequency lock system which works by detecting the resonance frequency of D₂O and compares it with the fixed frequency.
- Phase sensitive detector (Phase lock loop)



2.1.6 Shim system:

- Superconductive shim.
- Room temperature shim:
- Field distribution generated by a large number of coils are described a "spherical harmonic function" which has terms like Z^0 , Z^1 , Z^2 , X , Y , XY , ZX , ZY , ZXY .. etc and can be shimmed separately.

2.1.7 Transmitter and Pulse Generation:

Transmitter has 2-5 channels that allow the delivery of up to five frequencies to the probe. Each channel has a frequency generator, amplifier and filters. The transmitter frequency, or **carrier frequency of the RF-pulse, ω_{RF}** , is generated by mixing together two frequencies. The first frequency that contributes to the carrier frequency is **ω_{syn}** . This frequency is adjustable and is generated from the frequency synthesizer (SYN) under computer control. The second is an internal **constant frequency called the intermediate frequency, or ω_{IF}** . Electronic mixing of these two frequencies generates signals at two frequencies, **$\omega_{syn} + \omega_{IF}$ and $\omega_{syn} - \omega_{IF}$** . The higher frequency is retained and sent to the amplifier. The purpose of this mode of frequency generation is to provide a means to reduce electronic noise in the spectrum by adding to the detected signal a known offset frequency, **ω_{IF}** , that can be used to separate the real experimental signal from the noise.

The amplification and phase of the signal from the frequency synthesizer is under control of the computer. The amplification levels are specified in decibels as defined below:

$$dB = 10 \log \frac{P_1}{P_2} = 20 \log \frac{V_1}{V_2}$$

	3 dB	6dB	10dB	20dB	30dB
Voltage	$(2)^{1/2}$	2	$(10)^{1/2}$	10	$(1000)^{1/2}$
Power	2	4	10	100	1000
Pulse width	$(2)^{1/2}$	2	$(10)^{1/2}$	10	$(1000)^{1/2}$

Although the transmitter power is specified in dB, its value in published NMR experiments (pulse sequences) is generally given as the strength of the B₁ field, in Hz. Consequently, it is necessary to inter-convert between the two units. The B₁ field can be calculated from the length of the 90° pulse length, as follows: The flip angle, β, of a pulse of length τ, applied at a field strength of B₁, is: $\beta = \gamma B_1 \tau$. Selecting a flip angle of 90° and converting γB_1 to frequency units of Hz gives: $\pi/2 = 2\pi[\gamma B_1] \tau_{90}$

Therefore, the field strength in Hz (γB_1) is: $\gamma B_1 = 1/4 \tau_{90}$

For example, a 90° pulse of 10 μsec corresponds to a B₁ field strength of 25 kHz

2.1.7.1 Shaped Pulses:

Many RF-channels will contain an optional waveform generator, indicated as WFG that allows the production of pulses with arbitrary shapes. The pulse is divided into a number of small segments, and each segment possesses its own amplitude and phase. For example a Gaussian shaped pulse can be generated by simply varying the amplitude of each segment by the value of the Gaussian function. When the shaped pulse is applied, the phase and amplitude of each segment is used to control the output of the amplifier

2.1.8 Receiver:

Four frequencies :

ω_s : (signal); ω_{syn} : Synthesizer frequency;

ω_{IF} : Intermediate frequency: Set by the manufacturer (10 or 30 MHz for Bruker ?)

Same for all channels for easy for setting phase coherence or references.

ω_{RF} : Rotating frame frequency or frequency of the RF pulse.

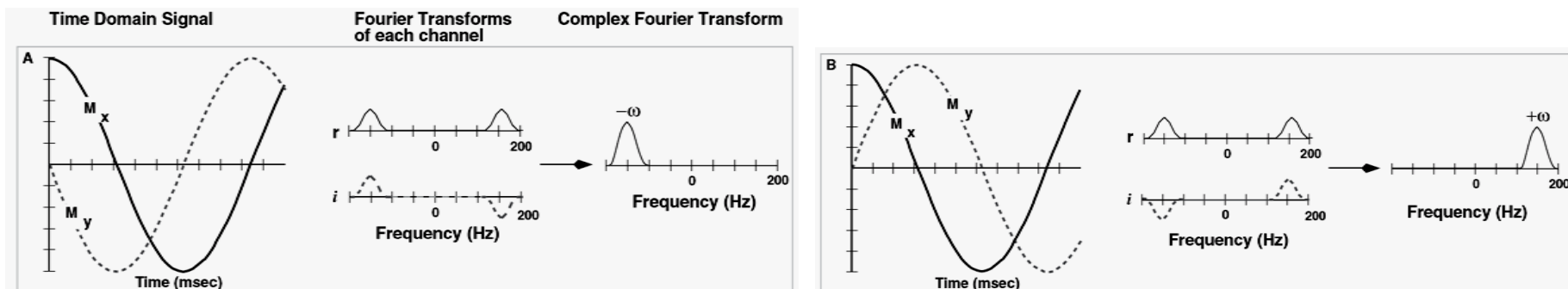
$\omega_{RF} = \omega_{syn} + \omega_{IF}$;

FID oscillating frequency (Audio frequency) = $\omega_s - \omega_{RF} = \omega_s - \omega_{syn} - \omega_{IF}$

2.1.9 Quadrature detection:

The individual mixers in each channel differ in the phase of the intermediate frequency that is mixed with the signal from the pre-amp, one is phase shifted by 90° relative to the other. The signals that are output from each mixer are either $\cos(\omega t)$ or $\sin(\omega t)$ and can be considered to be equivalent to the projection of the transverse magnetization on to the x- and y-axis, respectively, namely M_x and M_y .

$$M(t) = M_x + iM_y = \cos(\omega't)e^{-t/T_2} + i\sin(\omega't)e^{-t/T_2} = e^{i\omega't}e^{-t/T_2}$$



2.2 Acquiring a spectrum:

2.2.1 Sample preparation:

Sample quality, O₂ effect, Salt effect, , sample volume, sample susceptibility.

2.2.2 Beginning the Experiment

After the sample is inserted into the magnet the following steps should be performed before data acquisition occurs.

1. *Temperature equilibration:* Ideally, the sample should be in the probe for approximately 10 – 15 min to allow for thermal equilibrium to occur.
2. *Locking the spectrum on the deuterium line:* Locking may require adjustment of the lock frequency, power of the lock transmitter, and gain of the lock receiver.
3. *Adjustment of the lock phase:* This insures that a pure dispersion signal is available to the lock circuit for field stability.
4. *Shimming of the magnetic field:* This can be done either manually or with a computer automated algorithm.
5. *Tuning and matching of the probe:* This insures optimal transfer of the power from the transmitter to the sample.
6. *Calibration of pulses:* Transmitter power levels are measured to insure that the pulses are of the desired flip angle.

2.2.3 Temperature measurement:

Internal standard: Separation of the two peaks in methanol (CH₃OH)

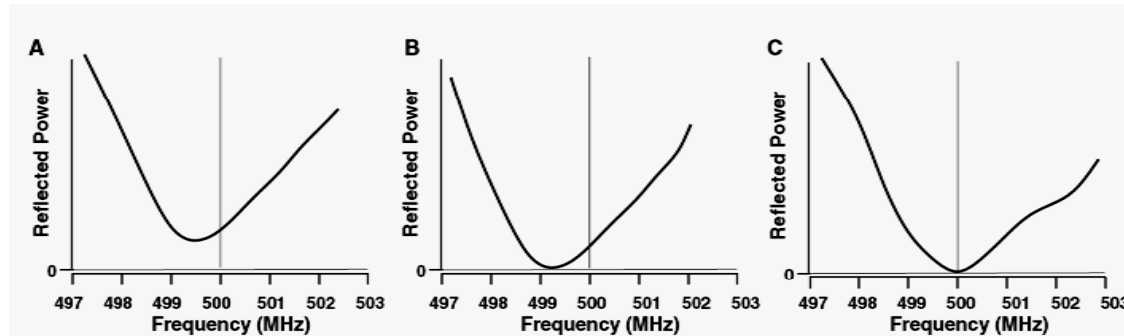
$$T = 403.0 - 29.53\Delta\delta - 23.87[\Delta\delta]^2$$

2.2.4 Shimming

2.2.5 Tuning and Matching the probe

Tuning: Adjust resonance freq

Matching: Adjust impedance, Z to 50 Ohms.



2.2.6 Adjusting the Transmitter:

Normally apply 90° pulse but it may not be the optimal angle if you repeat excitation faster than $3 \times T_1$.

2.2.6.1 Frequency and Power of the Transmitter:

The frequency of the transmitter, ω_{RF} , defines Ω , the rotation rate of the rotating coordinate frame. In our discussions of pulses in Chapter 1, it was assumed that the frequency of the excitation pulse was the same as the frequency of the nuclear spin transition and the 90° pulse cleanly tipped the magnetization from the z-axis to the xy plane. However, as the resonance line becomes further removed from the frequency of the RF-pulse, the efficiency of excitation decreases. This is due to the fact that the effective field, B_{eff} , becomes closer to the z-axis as resonance frequency becomes more distant from the transmitter frequency

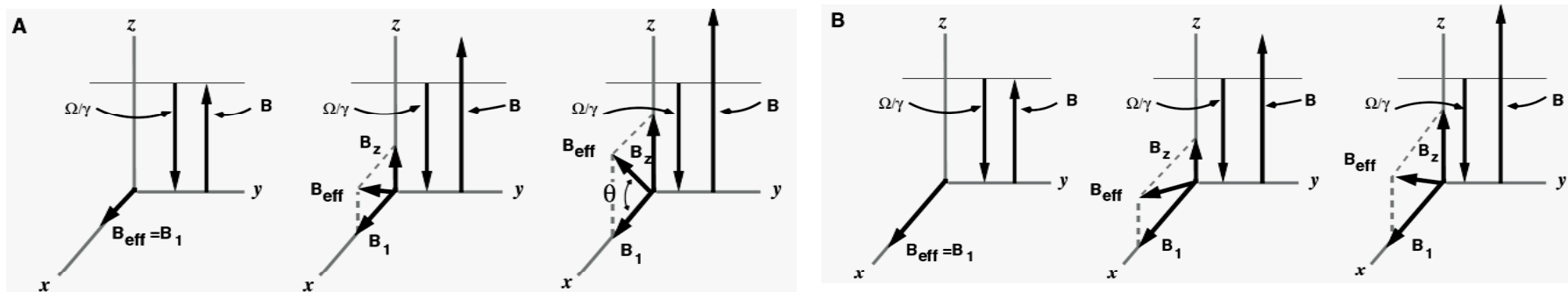
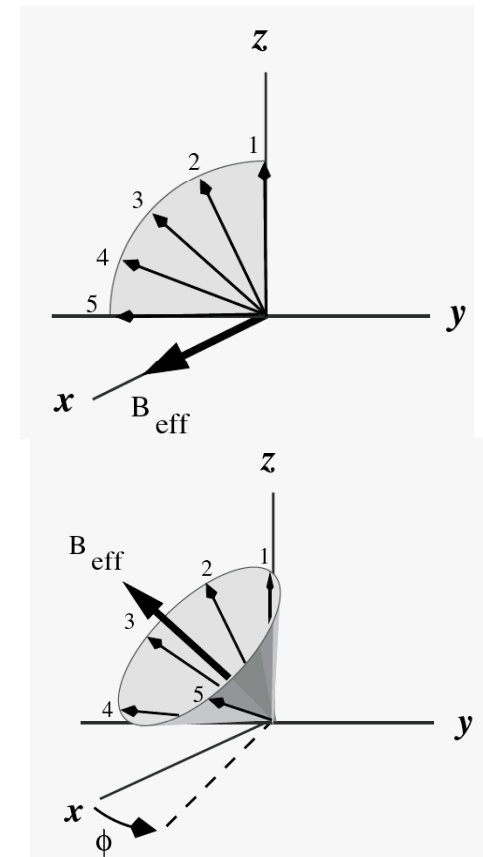


Figure 2.9. Effect of frequency offset and B_1 field strength on B_{eff} in the rotating frame. Panel A illustrates the effect of a weak B_1 field while panel B illustrates the effect of a strong B_1 field on B_{eff} . The leftmost section in each figure shows an on-resonance spin, the middle and right sections illustrate the effects of increasing the resonance offset on B_{eff} . The three fields present during the pulse are B_1 , along the x-axis in this example, Ω/γ , the fictitious field generated by the rotation of the coordinate frame, and B , the field felt by the spin at its nucleus ($B = (1 - \sigma)B_0$). The effective field of the pulse, indicated by B_{eff} , is the vector sum of all three fields. Note that Ω/γ is constant in all cases and is defined by the transmitter frequency. In contrast, the magnetic field at the nucleus, B , varies according to the resonance position of the line. When the rate of rotation of the coordinate frame equals the resonance frequency, $\Omega = \omega_s$, the two fields along the z-axis cancel and the B_{eff} is equal to B_1 (left diagrams in both A and B). Off-resonance, B_{eff} is tilted towards the z-axis by an angle θ . Note that for any given frequency offset, the tilt of B_{eff} towards the z-axis becomes more pronounced as the strength of the B_1 field decreases. At large resonance offsets ($B \gg \Omega/\gamma$), B_{eff} will be aligned along the z-axis and is completely ineffective at rotating the magnetization to the x-y plane.

$$(B_{eff} = \sqrt{B_1^2 + B_z^2})$$

The precession of the magnetization about the effective field is shown in Fig. 2.10. As before, for those spins that are on-resonance, the 90° x-pulse brings them to the y-axis. In contrast, those spins that are off-resonance ($\omega_s \neq \Omega$) will precess about B_{eff} for the same period of time, but the total angle that they precess will be always be greater than 90° because B_{eff} is always greater than B_1 ($B_{eff} = \sqrt{B_1^2 + B_z^2}$). After the pulse, the magnetic moment of off-resonance spins will be found either below or above the x-y plane, depending on the magnitude and orientation of B_{eff} . Therefore the amount of detectable magnetization in the x-y plane will decrease relative to an on-resonance spin. In addition to a loss of intensity, the bulk magnetization that is present in the x-y plane will be shifted away from the x-axis by an angle ϕ . Each of these effects will be discussed in more detail below.

Figure 2.10. Effect of on-resonance and off-resonance 90° x-pulses on the bulk magnetization. Precession of the bulk magnetization around B_{eff} is shown when the frequency of the pulse is on-resonance (top panel) and when it is off resonance (lower panel). The labeled arrows shown the path of the magnetization during the application of the pulse. In the case of the on-resonance pulse, the rotation angle is 90° about the x-axis, bringing the magnetization to the minus y-axis. In contrast, the off-resonance pulse rotates the magnetization by more than 90° about B_{eff} . Consequently, the bulk magnetization is found above the x-y plane after the pulse. The dotted line shows the projection of the final position on the x-y plane. The magnetization is also shifted by an angle ϕ from the x-axis.



Phase Effects: The shift of the transverse (x-y) magnetization from the x-axis by the angle ϕ , will produce a mixed lineshape that is a combination of absorption and dispersion lineshapes. This can be seen by considering the time domain signal associated with an off-resonance signal and its subsequent Fourier transform. The time domain signal is:

$$S(t) = e^{i\phi} e^{i\omega_s t} e^{-t/T_2} = [\cos(\phi) + i\sin(\phi)] e^{i\omega_s t} e^{-t/T_2} \quad (2.8)$$

Fourier transform of this signal gives:

$$F(\omega) = [\cos(\phi) + i\sin(\phi)] \left[\frac{T_2}{1 + T_2^2(\omega - \omega_s)^2} + i \frac{T_2^2(\omega - \omega_s)}{1 + T_2^2(\omega - \omega_s)^2} \right] \quad (2.9)$$

The real part (Observable) of this signal is:

$$\text{Absorption} \quad \cos(\phi) \frac{T_2}{1 + T_2^2(\omega - \omega_s)^2} - \text{Dispersion lineshape} \quad \sin(\phi) \frac{T_2^2(\omega - \omega_s)}{1 + T_2^2(\omega - \omega_s)^2} \quad (2.10)$$

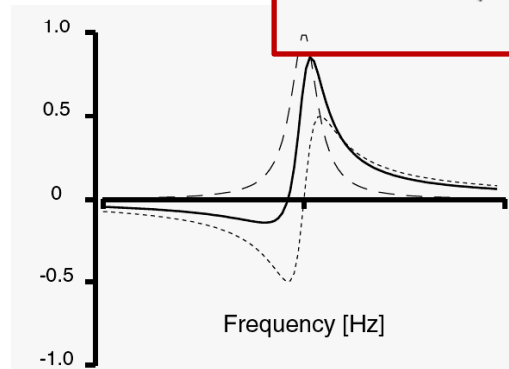


Figure 2.11 Effect of phase angle on the lineshape. Lineshapes are pure absorption ($\phi=0$, dashed line), mixed ($\phi=45^\circ$, solid line), and pure dispersion ($\phi=90^\circ$, dotted line).

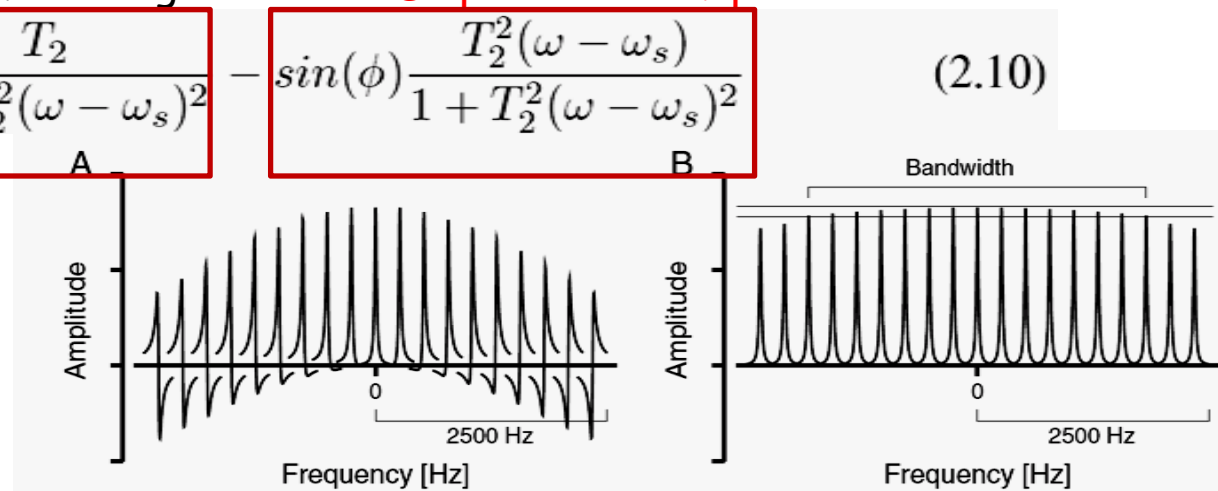


Figure 2.12. Effect of frequency offset on the phase and amplitude of resonances. Phase (Panel A) and amplitude changes (Panel B) as a function of the frequency difference between the resonance line and the carrier frequency. Panel (A) shows the NMR resonance line for different resonance offsets. When the offset is 2.5 kHz, the lineshape is pure dispersion, indicating that the magnetization is along the imaginary axis after the pulse. The right panel (B) shows the intensity of the resonance ($\sqrt{S_r^2 + S_i^2}$) as a function of the offset. The upper horizontal line indicates the maximum amplitude, which occurs when $\omega_s = \Omega = \omega_{RF}$. The lower horizontal line indicates the 95% level, which defines the bandwidth of the pulse. The 90° pulse length was $50 \mu\text{sec}$.

2.2.6.2 Selective Excitation

It is often desirable and necessary to excite only a defined region in the experiment. This can be accomplished by selective excitation using particularly shaped pulse or combination of crafted pulses.

2.2.7 Calibration of 90° pulse length

Precise excitation of spins is essential in complex experiment. One way to do this is to determine the 360° pulse length:

Calibration of a 360° Pulse

1. Place the transmitter on the strongest line in the spectrum.
2. Set the transmitter power to the desired level, usually full power.
3. Acquire a spectrum with a very short pulse length, $\approx 1\mu\text{sec}$.
4. Phase the spectrum to give a pure absorption line.
5. Increase the pulse length in small (1-2 μsec) steps until the maximum signal is observed, this is *approximately* a 90° pulse.
6. Apply a pulse that is four times the 90° pulse length. If the observed resonance is positive, the pulse was greater than 360°. If the resonance is negative, the pulse was shorter than 360°. Alter the pulse length accordingly until a null (zero) signal is obtained, indicating a 360° pulse.
7. Divide the 360° pulse length by four to obtain the 90° pulse length. A final accuracy of 0.1 μsec is usually sufficient.

2.2.7.1 Placement of the Carrier

Place the strong solvent at the center by setting the carrier frequency at the solvent resonance frequency.

2.2.8 Setting the Sweepwidth (SW): Dwell Times and Filters

2.2.8.1 Dwell Time. $SW = 1/\tau_{dw}$

2.2.8.2 Folding and Aliasing:

Nyquist theorem: $1/\tau_{DW}$ must be larger than f_{max} where f_{max} is the frequency of the resonance which is furthest from the reference frequency.

Nyquist frequency: $f_N = 1/(2\tau_{dw})$

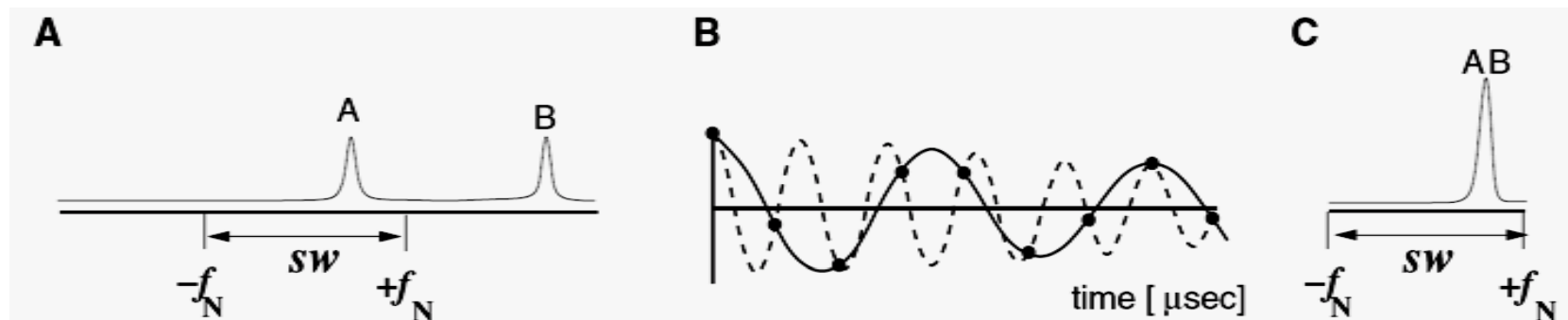
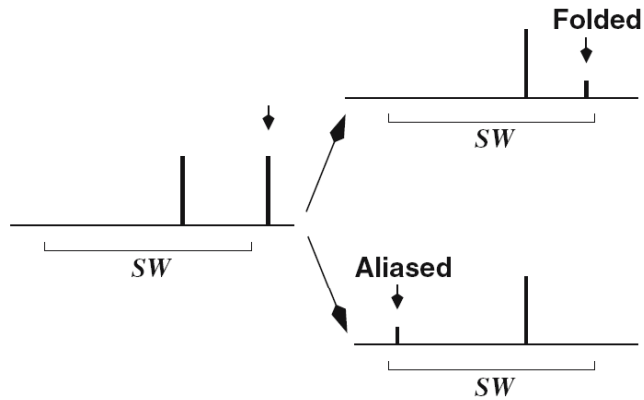


Figure 2.13. Nyquist frequency and folding of spectral lines. The true NMR spectrum of a sample is shown in Panel A (left). Two resonance lines are present, “A” and “B”. The experimental spectral width, defined by the dwell time, is indicated below the spectrum. The lowest and highest frequencies correspond to the Nyquist frequency, f_N . The analog FID that would be detected from these two resonances is shown in Panel B (center). The solid line is the FID from resonance “A” and the dotted line is the FID from resonance “B”. The dots indicate the points that are sampled during digitization of the FID. Since both resonances give exactly the same digital FID, they will have the same frequency in the transformed spectrum.



The observed position in the spectrum of a resonance that lies outside of the sweepwidth depends on whether the data were collected as a single channel, such as $\cos(\omega t)$, or in quadrature ($S(t) = \cos(\omega t) + i\sin(\omega t)$). Single channel detection will produce a folded peak, while quadrature detection will produce an aliased

Folding: A peak with a frequency $f_N + \delta$ will appear at a frequency of $f_N - \delta$.

This effect is called folding because the peak outside of the sweepwidth has been folded, or reflected, about the edge of the spectrum.

Aliasing: A peak with a frequency of $f_N + \delta$ will appear at a frequency of $-f_N + \delta$.

This is referred to as aliasing. Note that in this case the relative frequencies of the peaks have been maintained, but they have been shifted by a multiple of the sweepwidth.

Explanation of these two effect is in the text and will not be explained here.

2.2.8.3 Receiver filter: Bandpass filters are usually set at at bandwidth equals toe SW so as to attenuate the signal outside the region of interest. But in multi-dimensional expt it is not set that way and the aliased signals are fold back in full intensities.

2.2.9 Setting the Receiver Gain

Too high or too low will produce signal distortion. (Place strongest signal to full scale)

Resolution of an analog-to-digital converter (ADC): x bit ADC.

N bit ADC means divide the full signal into 2^N divisions. Example: 4 bit ADC will have resolution of $5V/2^4 = 0.3125$ Volts /division for a full signal of 5 Volts. Any signal lower than 0.3125 V will be treated as 0 and cannot be detected. But if the signal is detected with a 10 bit ADC the resolution will be $5/2^{10} \sim 0.005$ V. The higher the ADC resolution the better we can detect weak signal.

Water concentration: 110 M and sample concentration: 1 mM (About 10^{-5} of water signal)

ADC bit needed: 17 bit → Water (solvent) signal suppression is needed.

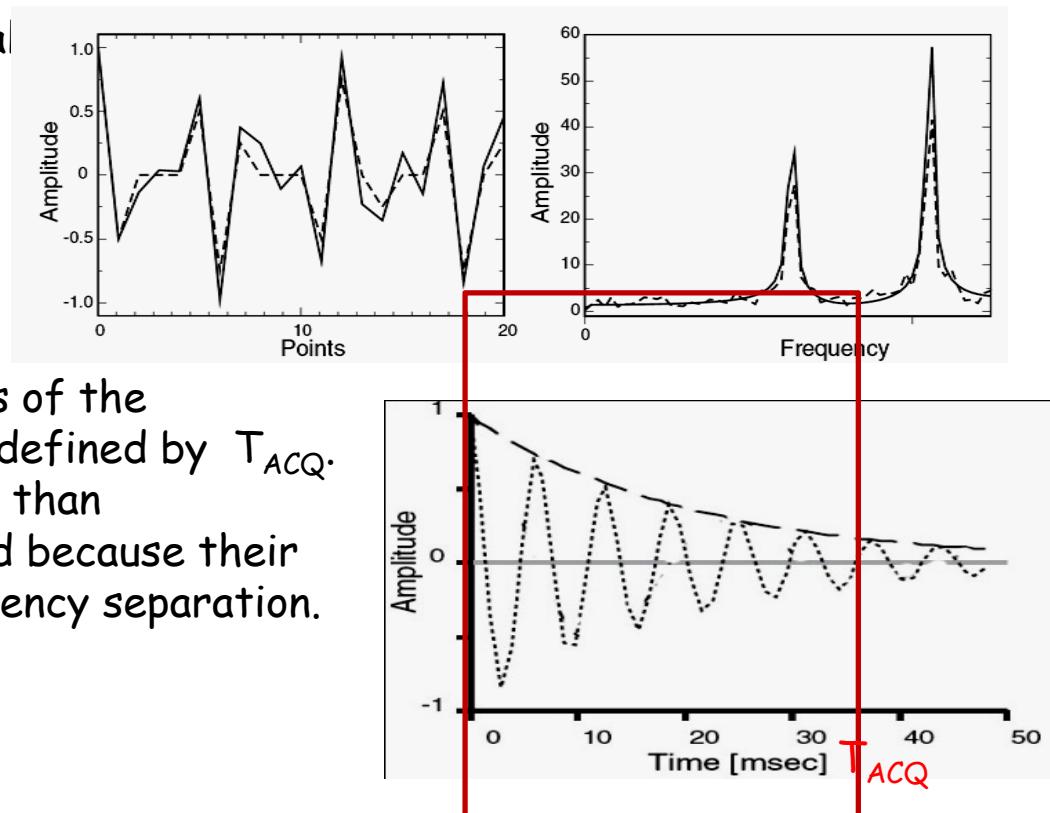
2.2.10 Spectral Resolution and Acquisition Time of FID

Spectral resolution depends on the total acquisition time (T_{ACQ}):

$$T_{ACQ} = \text{number of points} \times DW$$

The true, or actual, resolution of the spectrum is defined by the *observed Linewidths* of the resonances, which depends on both the intrinsic linewidths of the resonances and the spectral resolution defined by T_{ACQ} . Consequently, any peaks that are closer than $\approx 1/(\pi T^2) + 2/T_{ACQ}$ cannot be resolved because their observed linewidths exceed their frequency separation.

Digital resolution: SW/N



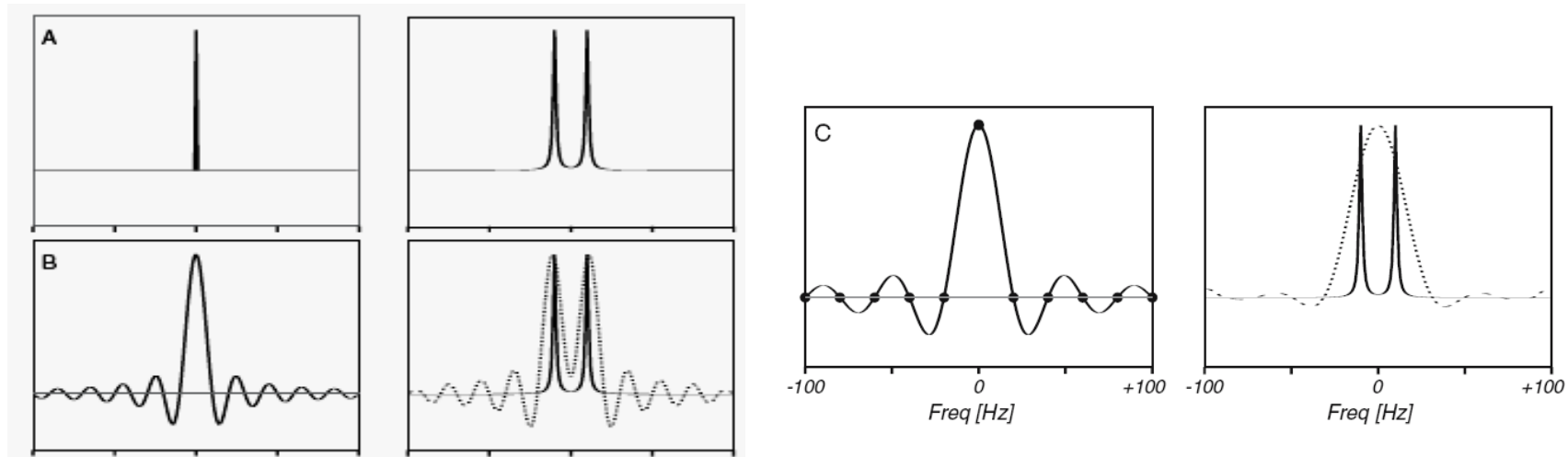


Figure 2.18. Acquisition time and spectral resolution. The effect of the acquisition time on the corresponding to increasingly shorter acquisition times. The peak separation is 20 Hz and the intrinsic linewidths of each peak is 2 Hz. Rows A, B, and C represent acquisition times of 2 sec, 100 msec, and 50 msec, respectively. The left panels show the Fourier transform of the square waves that corresponds to each acquisition time. The right panels show the true spectra as solid lines and the convolution of the spectra with the sinc function as dotted lines. When the acquisition time is 2 sec (A), there is essentially no additional broadening of the resonances by the convolution with the sinc function. When an acquisition time of 100 msec is used (B), the lines are broadened by approximately 20 Hz, but they are still resolved. When the signal is acquired for only 50 msec, the additional broadening is approximately 40 Hz and the individual lines are no longer resolved. The 'wiggle' patterns that are introduced to the spectra by the transform of the square wave may not be observed in the final spectrum because the sampling frequency of the spectrum (SW/n) is such that only the zero-crossing points of the sinc function are sampled (see Panel C). Increasing the digital resolution, by adding more points, will cause these wiggles to appear in the spectrum.

2.2.10.1 Scan Repetition Rate:

The steady state signal for a repetition rate of T is: $A \approx A_o(1 - e^{-T/T_1})$

The Optimal pulse angle depends on the ratio of the scan repetition rate to spin-lattice relaxation time according to the following equation, derived by Ernst et al [53]:

$$\cos \beta_{opt} = e^{-T/T_1}$$

Dummy scan: The scans for establishing steady state before data acquisition.

2.3 Experimental 1D-pulse Sequence: Pulse and Receiver phase

2.3.1. Phase Cycle

2.3.1.1 Phase of the RF-pulse:

$$P_x = \cos(\omega t) = \frac{1}{2} [e^{i\omega t} + e^{-i\omega t}]$$